SUPPLEMENTARY MATERIAL

Micro-Raman Spectroscopy Reveals the Presence of Octacalcium Phosphate and Whitlockite in Association with Bacteria-Free Zones Within the Mineralized Dental Biofilm

Brief title:

Revisiting the Mineralized Dental Biofilm

Furqan A. Shah

Department of Biomaterials, Sahlgrenska Academy, University of Gothenburg, Göteborg, Sweden

Author for correspondence:

Department of Biomaterials,

Sahlgrenska Academy, University of Gothenburg,

Box 412, SE-405 30, Göteborg, Sweden

Tel: +46 31 786 28 98; Email: furqan.ali.shah@biomaterials.gu.se

http://orcid.org/0000-0002-9876-0467

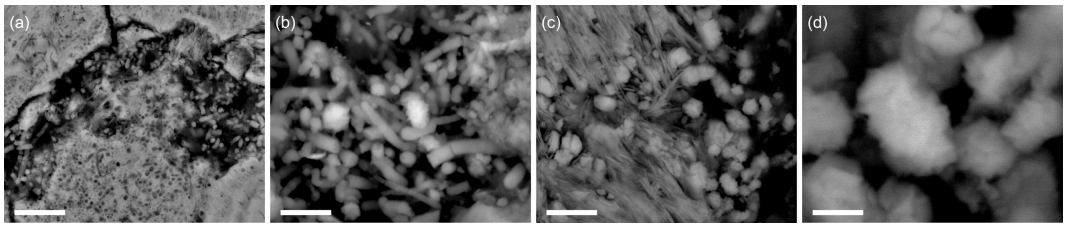

Fig. S1: Backscattered electron scanning electron microscopy. (a) Bacteria-containing zone (Bact+) showing mineralized bacteria and partial extramicrobial mineralization. (b) Intramicrobial mineralization is seen as smooth, solid mineral deposits resembling the morphologies of bacteria found in dental plaque. (c) Bacteria-free zone (Bact–) showing mineral platelets and micrometer-sized mineral nodules. (d) The mineral nodules appear considerably less smooth than mineralized bacteria. Scale bars in a = 10 μm; b, c = 5 μm; and d = 1 μm.

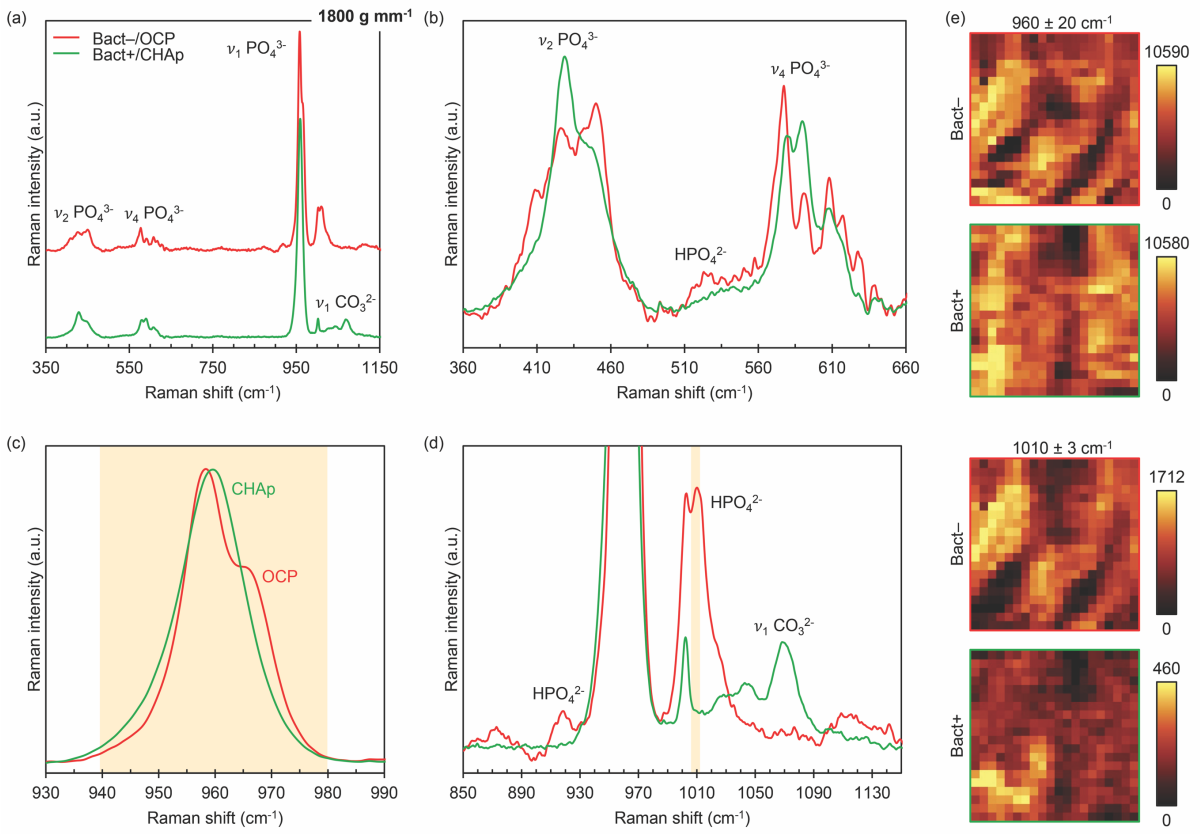

Fig. S2: Raman spectroscopy. (a) Average spectra of Bact+ and Bact– (1,800 g mm^{-1} grating, 317–1,423 cm^{-1} spectral range, spectral center at 900 cm^{-1}, 10 s integration time per pixel). Bact+ are comprised of carbonated apatite (CHAp). Bact– are predominantly made up of octacalcium phosphate (OCP). 5 µm × 5 µm ROI, 400 spectra; (n = 2). (b) Detail of the 360–660 cm^{-1} region (ν_2 PO_4^{3-} and ν_4 PO_4^{3-}). (c) Detail of the 930–990 cm^{-1} region (ν_1 PO_4^{3-}; normalized intensities). (d) Detail of the 850–1,150 cm^{-1} region (HPO_4^{2-}, ν_1 CO_3^{2-}). (e) The example shows Raman maps of ν_1 PO_4^{3-} (960 ± 20 cm^{-1}) and HPO_4^{2-} (1,010 ± 3 cm^{-1}) in Bact+ and Bact–. Bact+ exhibit very low HPO_4^{2-} signal, indicating the absence of OCP. At Bact–, HPO_4^{2-} signal is significantly higher (vs. Bact+) and the spatial distribution closely follows that of ν_1 PO_4^{3-}. The color scale bars show charge-coupled device (CCD) detector counts.

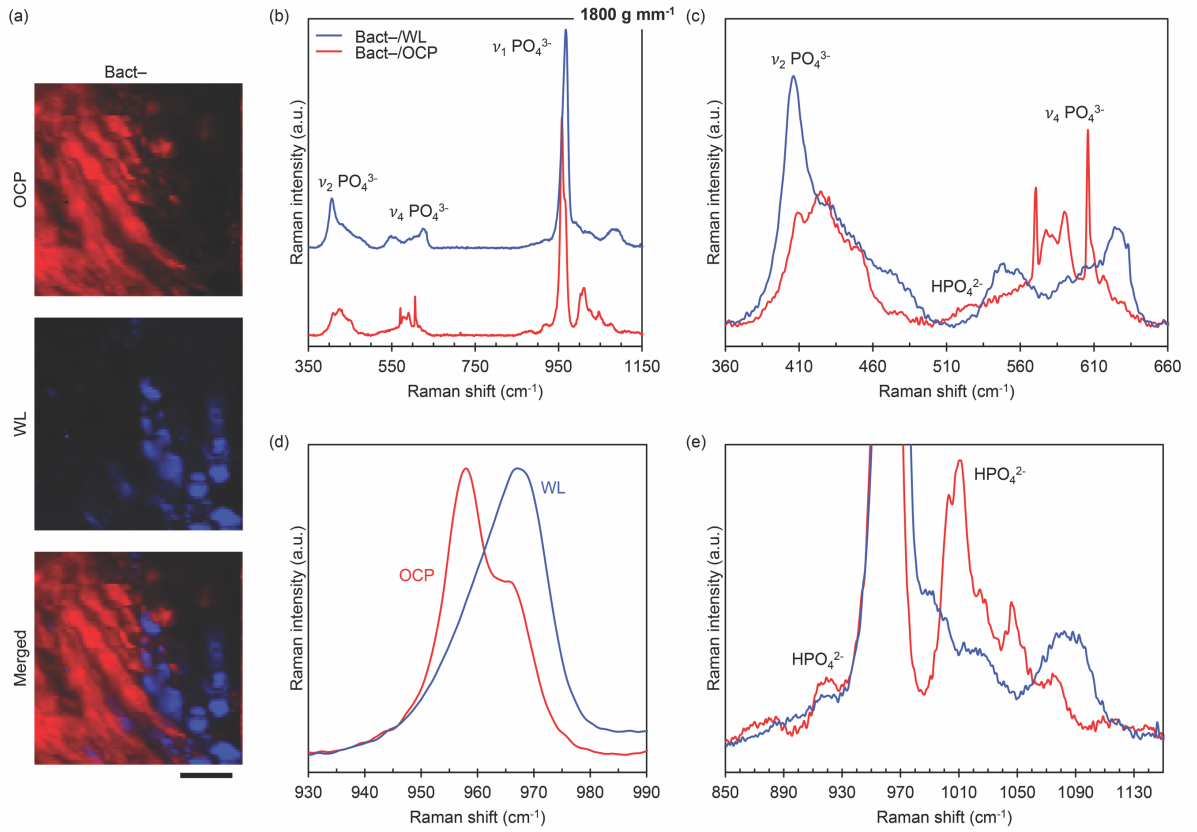

Fig. S3: Raman spectroscopy. (a) Raman maps of octacalcium phosphate (OCP), whitlockite (WL), and color-merge of OCP (red) and WL (blue) in Bact–. 20 µm × 20 µm ROI, 6,400 spectra. (b) OCP and WL spectra corresponding to the Raman maps (shown in a). (c) Detail of the 360–660 cm^{-1} region (ν_2 PO_4^{3-} and ν_4 PO_4^{3-}). (d) Detail of the 930–990 cm^{-1} region (ν_1 PO_4^{3-}; normalized intensities). (e) Detail of the 850–1,150 cm^{-1} region (HPO_4^{2-}, ν_1 CO_3^{2-}). Scale bar in a = 5 µm.

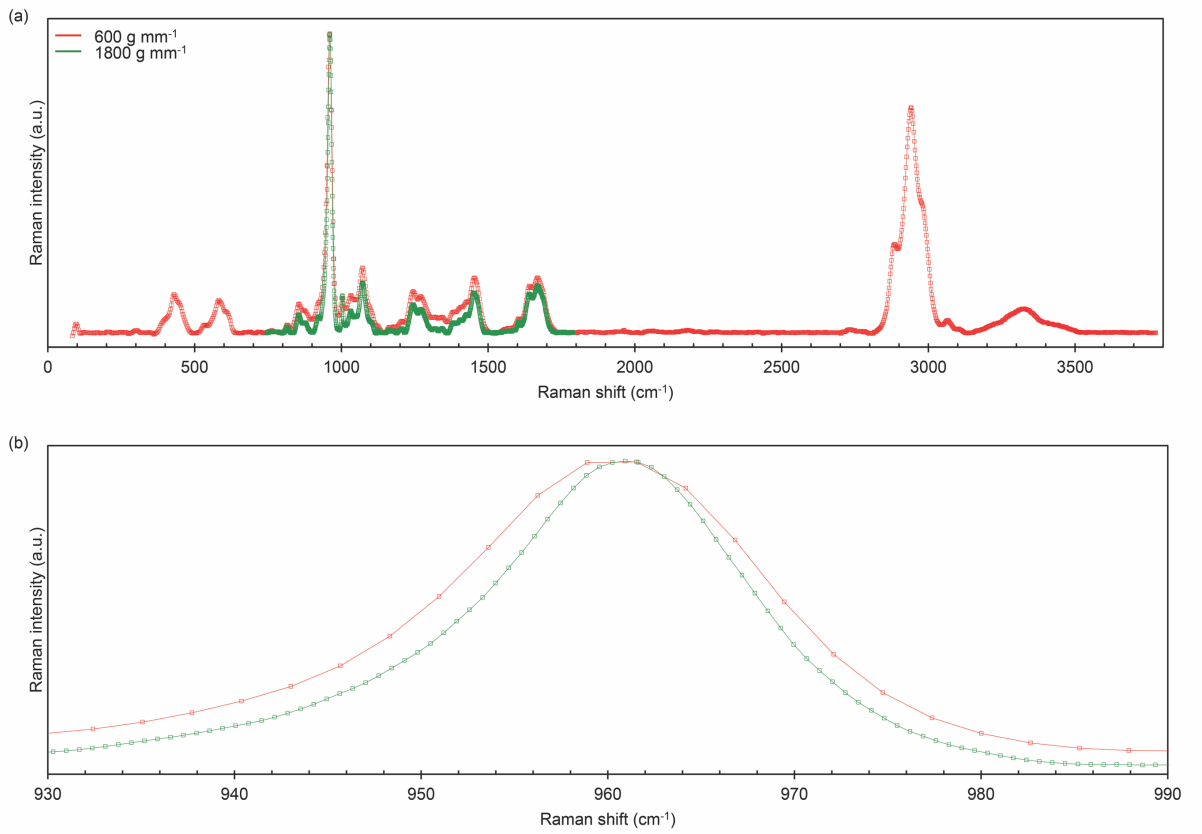

Fig. S4: Comparison of spectral range and spectral resolution achieved with 600 g mm^{-1} and 1,800 g mm^{-1} gratings. (a) The example shows average spectra of native bone. The spectral range of the 600 g mm^{-1} (84–3,775 cm^{-1} spectral range; spectral center at 2,150 cm^{-1}) is significantly broader than the 1,800 g mm^{-1} grating (745–1,790 cm^{-1} spectral range; spectral center at 1,250 cm^{-1}). (b) Due to a smaller step-size, high resolution spectra allow detection of fine features, e.g., peak broadening, peak shifts, and band splitting, such as of the ν_1 PO_4^{3-} peak (here, centered around 960 cm^{-1}).

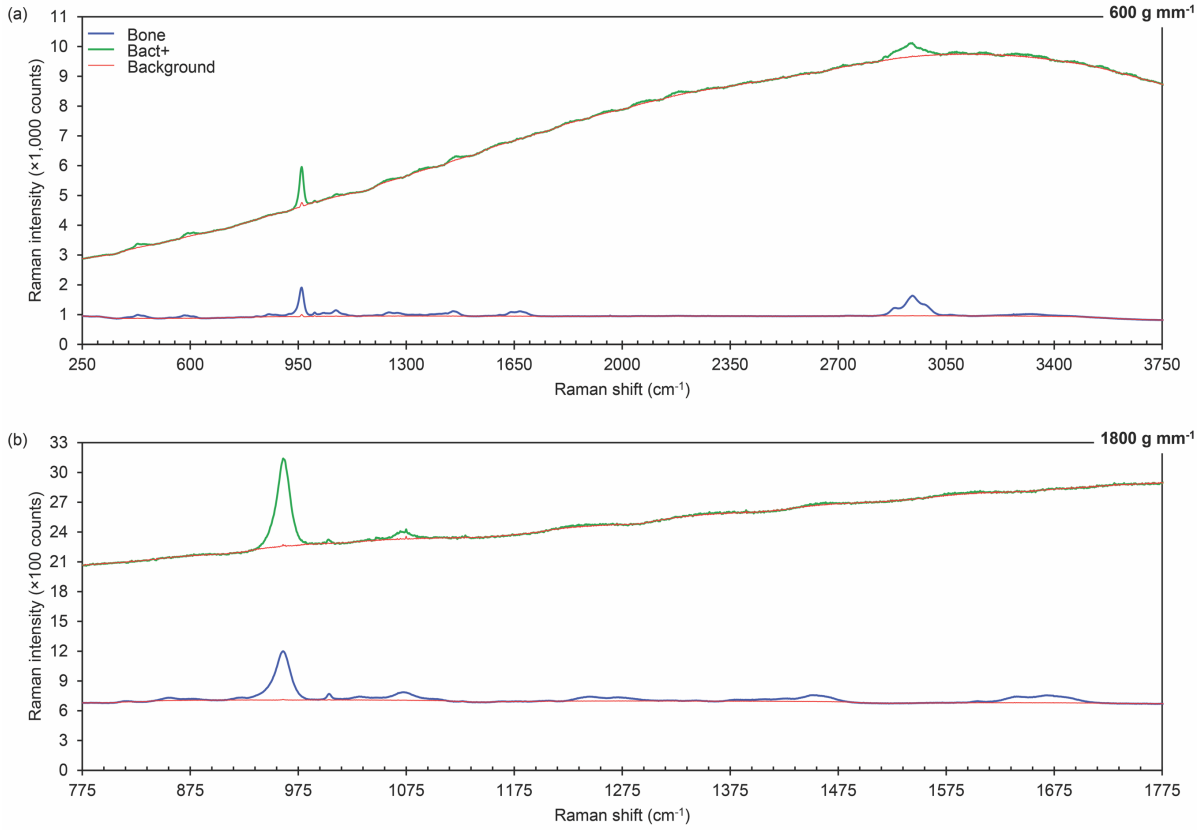

Fig. S5: Background fluorescence emission by Bact+ and native bone. (a–b) Bact+ generate significantly higher background fluorescence than native bone with both 600 g mm^{-1} (a) and 1,800 g mm^{-1} (b) gratings. Compared to native bone, the background fluorescence emission from Bact+ increases dramatically at higher wavenumbers.